OPEN ACCESS Freely available online

PLOS ONE

Characterization of the Prostate-Specific Antigen (PSA) Catalytic Mechanism: A Pre-Steady-State and Steady-State Study

Luigi Tomao[1], Diego Sbardella[2,3], Magda Gioia[2,3], Alessandra Di Masi[1,4], Stefano Marini[2,3], Paolo Ascenzi[1,4], Massimo Coletta[2,3]*

1 Department of Sciences, University of Roma Tre, Roma, Italy, **2** Department of Clinical Sciences and Translational Medicine, University of Roma "Tor Vergata", Roma, Italy, **3** Interuniversity Consortium for the Research on Chemistry of Metals in Biological Systems, Bari, Italy, **4** Interdepartmental Laboratory of Electron Microscopy, University of Roma Tre, Roma, Italy

Abstract

Prostate-specific antigen (PSA), an enzyme of 30 kDa grouped in the kallikrein family is synthesized to high levels by normal and malignant prostate epithelial cells. Therefore, it is the main biomarker currently used for early diagnosis of prostate cancer. Here, presteady-state and steady-state kinetics of the PSA-catalyzed hydrolysis of the fluorogenic substrate Mu-His-Ser-Ser-Lys-Leu-Gln-AMC (spanning from pH 6.5 to pH 9.0, at 37.0°C) are reported. Steady-state kinetics display at every pH value a peculiar feature, represented by an initial "burst" phase of the fluorescence signal before steady-state conditions are taking place. This behavior, which has been already observed in other members of the kallikrein family, suggests the occurrence of a proteolytic mechanism wherefore the acylation step is faster than the deacylation process. This feature allows to detect the acyl intermediate, where the newly formed *C*-terminal carboxylic acid of the cleaved substrate forms an ester bond with the -OH group of the Ser195 catalytic residue, whereas the AMC product has been already released. Therefore, the pH-dependence of the two enzymatic steps (*i.e.*, acylation and deacylation) has been separately characterized, allowing the determination of pK_a values. On this basis, possible residues are tentatively identified in PSA, which might regulate these two steps by interacting with the two portions of the substrate.

Citation: Tomao L, Sbardella D, Gioia M, Di Masi A, Marini S, et al. (2014) Characterization of the Prostate-Specific Antigen (PSA) Catalytic Mechanism: A Pre-Steady-State and Steady-State Study. PLoS ONE 9(7): e102470. doi:10.1371/journal.pone.0102470

Editor: Alessio Lodola, University of Parma, Italy

Received May 9, 2014; **Accepted** June 19, 2014; **Published** July 28, 2014

Data Availability: The authors confirm that all data underlying the findings are fully available without restriction. All relevant data are within the paper and its related figures.

Funding: This work was financially supported by the Italian Ministery of University and Research (MiUR 265 PRIN 200993WWF_003 to M.C. and CLA 2014 to P.A). The funders had no role in study design, data collection and analysis, decision to publish, or preparation of the manuscript.

Competing Interests: The authors have declared that no competing interests exist.

* Email: coletta@seneca.uniroma2.it

Introduction

Prostate-specific antigen (PSA), an enzyme of 30 kDa grouped in the kallikrein family and also known as kallikrein-related peptidase 3 (KLK3) [1], is synthesized to high levels by normal and malignant prostate epithelial cells and, under pathological conditions, it is abundantly secreted in the extracellular compartments. For this reason, it is the main biomarker currently used for early diagnosis of prostate cancer. Therefore, serum levels of PSA are also useful to detect eventual recurrent forms and to follow up treatment response in not operable and metastatic tumors [2].

Like all other members of the kallikrein family, PSA is a serine protease that is synthesized in an inactive form as a zymogen which is composed of a pre-peptide (also known as signal peptide) and a pro-peptide (which maintains the enzyme in the latent form). Inside the epithelial cell, the 17 amino acid pre-sequence is first cleaved off by signal peptidases. Afterwards, in the extracellular environment, the additional 7 amino acid pro-sequence is removed by human kallikrein 2 (hK2) [3]. PSA shows a conserved position of the Asp102/His57/Ser195 catalytic triad [4] (see Fig. 1). However, unlike most of kallikreins, which display a trypsin-like proteolytic specificity (*i.e.*, they cleave on the carboxyl side of a positively charged amino acid residue, namely Arg and Lys), PSA shows instead a chymotrypsin-like substrate specificity (*i.e.*, it cleaves on the carboxyl side of a hydrophobic amino acid residue, namely Tyr, Phe, Trp, and Leu). In addition, PSA is the only member of the kallikrein family that catalyzes the cleavage of substrates displaying the Gln residue at the P_1 position [5].

Prostate cancer can increase the amount of PSA released into the blood stream, even though serum PSA is kept inactive in a variety of different forms. As a matter of fact, serum PSA falls into two general categories, namely: (*i*) free PSA, which includes all the unbound zymogen forms, and (*ii*) complexed PSA, where also active forms are kept latent through the binding of serum protease inhibitors. Notably, PSA present in the extracellular fluid, surrounding prostate epithelial cells, has been reported to be enzymatically active, suggesting that its proteolytic activity plays a role in the physiopathology of prostate cancer [6].

The most important physiological substrates for PSA have been proposed to be semenogelin I (SgI) and semenogelin II (SgII). These proteins are synthesized and secreted by the seminal vesicles in spermatic fluid and are involved in the formation of a gel matrix

A

```
PSA       ---------------IVGGWECEKHSQPWQVLVA---SRGRAVCGGVLVHPQWVLTAAHC   42
KLK1      ---------------IVGGWECEQHSQPWQAALY---HFSTFQCGGILVHRQWVLTAAHC   42
KLK2      ---------------IVGGWECEKHSQPWQVAVY---SHGWAHCGGVLVHPQWVLTAAHC   42
KLK4      ---------------IINGEDCSPHSQPWQAALV---MENELFCSGVLVHPQWVLSAAHC   42
KLK6      ---------------LVHGGPCDKTSHPYQAALY---TSGHLLCGGVLIHPLWVLTAAHC   42
KLK7      ---------------IIDGAPCARGSHPWQVALL---SGNQLHCGGVLVNERWVLTAAHC   42
HPK       ---------------IVGGTNSSWGEWPWQVSLQVKLTAQRHLCGGSLIGHQWVLTAAHC   45
                          :: *  .   . *:*. :          *.* *:   ***:****
BCTRP     CGVPAIQPVLSGLARIVNGEDAVPGSWPWQVSLQ--DSTGFHFCGGSLISEDWVVTAAHC   58

PSA       IRN-----KSV-ILLGRHSLFHPED-TGQVFQVSHSFPHPLYDMSLLKNRFLRPGDDSSH   95
KLK1      ISD-----NYQ-LWLGRHNLFDDEN-TAQFVHVSESFPHPGFNMSLLENHTRQADEDYSH   95
KLK2      LKK-----NSQ-VWLGRHNLFEPED-TGQRVPVSHSFPHPLYNMSLLKHQSLRPDEDSSH   95
KLK4      FQN-----SYT-IGLGLHSLEADQEPGSQMVEASLSVRHPEYNRP----------LLAN   85
KLK6      KKP-----NLQ-VFLGKHNLRQRES-SQEQSSVVRAVIHPDYDAA----------SHDQ   84
KLK7      KMN-----EYT-VHLGSDTLGDR---RAQRIKASKSFRHPGYSTQ----------THVN   82
HPK       FDGLPLQDVWR-IYSGILNLSDITK-DTPFSQIKEIIIHQNYKVS----------EGNH   92
                     :  *  .*                  . *  :.              .
BCTRP     GVT-----TSDVVVAGEFDQGLET-EDTQVLKIGKVFKNPKFSIL----------TVRN   101

PSA       HLMLLRLSEPAE-LTDAVKVMDLPTQE--PALGTTCYASGWGSIEPEEFLTPKKLQCVDL   152
KLK1      HLMLLRLTEPADTITDAVKVVELPTQE--PEVGSTCLASGWGSIEPENFSFPDDLQCVDL   153
KLK2      HLMLLRLSEPAK-ITDVVKVLGLPTQE--PALGTTCYASGWGSIEPEEFLRPRSLQCVSL   152
KLK4      HLMLIKLDESVS-ESDTIRSISIASQC--PTAGNSCLVSGWGLLAN--GRMPTVLQCVNV   140
KLK6      HIMLLRLARPAK-LSELIQPLPLERDC--SANTTSCHILGWGKTADGD--FPDTIQCAYI   139
KLK7      HLMLVKLNSQAR-LSSMVKKVRLPSRC--EPPGTTCTVSGWGTTTSPDVTFPSDLMCVDV   139
HPK       HIALIKLQAPLN-YTEFQKPICLPSKGDTSTIYTNCWVTGWGFSKE-KGEIQNILQKVNI   150
          *: *::*       :.  : : :           ..*   ***             : . :
BCTRP     HITLLKLATPAQ-FSETVSAVCLPSADEDFPAGMLCATTGWGKTKYNALKTPDKLQQATL   160

PSA       HVISNDVCAQVHPQ-KVTKFMLCAGRWTGGKSTCSGDSGGPLVCNG----VLQGITSWGS   207
KLK1      KILPNDECKKVHVQ-KVTDFMLCVGHLEGGKDTCVGDSGGPLMCDG----VLQGVTSWGY   208
KLK2      HLLSNDMCARAYSE-KVTEFMLCAGLWTGGKDTCGGDSGGPLVCNG----VLQGITSWGP   207
KLK4      SVVSEEVCSKLYDP-LYHPSMFCAGGGQDQKDSCNGDSGGPLICNG----YLQGLVSFGK   195
KLK6      HLVSREECEHAYPG-QITQNMLCAGDEKYGKDSCQGDSGGPLVCGD----HLRGLVSWGN   194
KLK7      KLISPQDCTKVYKD-LLENSMLCAGIPDSKKNACNGDSGGPLVCRG----TLQGLVSWGT   194
HPK       PLVTNEECQKRYQDYKITQRMVCAGYKEGGKDACKGDSGGPLVCKHNGMWRLVGITSWGE   210
           ::  : * : :        *.*.*     *.:* *******:*       * *:.*:*
BCTRP     PIVSNTDCRKYWGS-RVTDVMICAGA--SGVSSCMGDSGGPLVCQKNGAWTLAGIVSWGS   217

PSA       EPCALPERPSLYTKVVHYRKWIKDTIVANP---------  237
KLK1      VPCGTPNKPSVAVRVLSYVKWIEDTIAENS---------  238
KLK2      EPCALPEKPAVYTKVVHYRKWIKDTIAANP---------  237
KLK4      APCGQVGVPGVYTNLCKFTEWIEKTVQAS----------  224
KLK6      IPCGSKEKPGVYTNVCRYTNWIQKTIQAK----------  223
KLK7      FPCGQPNDPGVYTQVCKFTKWINDTMKKHR---------  224
HPK       -GCARREQPGVYTKVAEYMDWILEKTQSSDGKAQMQSPA  248
            *.    *.: ..:  : .** ..
BCTRP     STCST-STPAVYARVTALMPWVQETLAAN----------  245
```

B

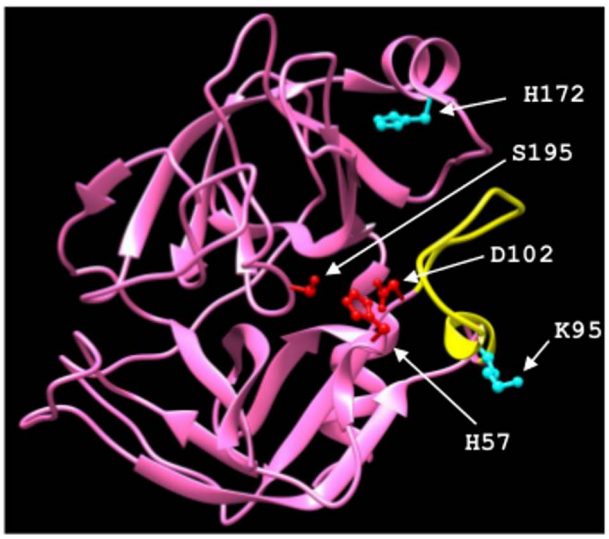

Figure 1. Sequence alignment of human kallikreins (panel A) and three-dimensional structure of PSA (panel B). Sequence alignment (panel A) is built with those human kallikreins for which the three-dimensional structure is available at the Protein Data Bank. The protein sequences were obtained from the NCBI database (http://www.ncbi.nlm-nih.gov). The progressive multiple alignment of PSA (also named kallikrein 3; NCBI entry number: CAD30845.1), kallikrein 1 (also named tissue kallikrein; KLK1; NCBI entry number: AAH05313.1), kallikrein 2 (KLK2; NCBI entry number: AAF08276.1), kallikrein 4 (KLK4; NCBI entry number: AAD38019.1), kallikrein 6 (KLK6; NCBI entry number: AAP35498.1), kallikrein 7 (KLK7; NCBI entry number: NP_644806.1), and human plasma kallikrein (HPK; NCBI entry number: AAF79940.1) was performed by the Clustal-Omega program (http://www.ebi.ac.uk/Tools/msa/clustalo). Only the trypsin-like serine protease domain of HPK has been aligned. The "*" symbol means that the residues are identical in all the aligned sequences; the ":" symbol indicate conserved substitutions, and the "." symbol means semi-conserved substitutions. The amino acid sequence of bovine chymotrypsinogen (BCTRP; NCBI entry number: 681083A) has been reported as the template. Three-dimensional structure of PSA (panel B). In both panels, the image was produced using UCSF Chimera molecular graphics package [26]. The "kallikrein loop" is in yellow [24,27,28], amino acid residues forming the catalytic triad are in red, and amino acid residues affecting the pH dependence of the catalytic parameters are in cyan.
doi:10.1371/journal.pone.0102470.g001

that wraps around ejaculated spermatozoa, preventing their functionalization (mainly via inhibition of reactive oxygen species) [7]. The gel matrix breaks down under the PSA enzymatic action, facilitating the spermatozoa movements [8]. PSA cleaves preferentially the Tyr-Glu peptide bonds and generates multiple soluble fragments of SgI and SgII [9] that seem to be the main antibacterial components in human seminal plasma [10]. These findings, together with the ability of PSA to process a number of growth regulatory proteins that are important in cancer growth and survival (such as Insulin-like growth factor binding protein, Parathyroid hormone-related protein, latent Transforming growth factor-beta 2 as well as extracellular matrix components, like fibronectin and laminin) [11-14], indeed suggest that PSA can facilitate tumor growth and metastasis dissemination [3,15,16]. On the other hand, PSA has been reported to slow down blood vessel formation, thus playing likely an important role in slowing the growth of prostate cancer [17]. As a whole, although currently PSA is a biomarker, its role in the pathobiology of prostate cancer remains obscure [3].

In view of the PSA importance both from the physiological and the pathological viewpoints, the present study is focused on insights into the catalytic mechanism of PSA. In particular, it has been investigated the PSA-catalyzed hydrolysis of the fluorogenic substrate Mu-His-Ser-Ser-Lys-Leu-Gln-AMC (Mu-HSSKLQ-AMC), a PSA-specific substrate designed on the basis of a PSA cleavage map for SgI and SgII [18]. Under pre-steady-state and steady-state conditions, the release of the Mu-HSSKLQ product (*i.e.*, the deacylation process) is the rate-limiting step of catalysis. The independent analysis of the pH dependence of the acylation and deacylation steps allows to determine the pK_a values of residues involved in the modulation of the proteolytic activity.

Materials and Methods

PSA (pure grade >96%), obtained from seminal fluid, was purchased by SunnyLab (SCIPAC Ltd, Sittingbourne, UK). The highly-specific PSA fluorogenic substrate Mu-HSSKLQ-AMC (purity >97%) was purchased from Sigma-Aldrich (Buchs, Switzerland).

The PSA-catalyzed hydrolysis of Mu-HSSKLQ-AMC was monitored spectrofluorimetrically at 460 nm with a Cary Eclipe spectrofluorimeter (Varian, Palo Alto, Ca, USA). The excitation wavelength was 380 nm with a slit bandwidth of 5 nm. The Mu-HSSKLQ-AMC concentration ranged between 5 and 70 μM, whereas the PSA concentration was 50 nM for all determinations. The PSA-catalyzed hydrolysis of Mu-HSSKLQ-AMC was investigated between pH 6.5 and 9.0 using the following buffers: 25 mM bis-tris-HCl and 25 mM tris-HCl, in the presence of 100 mM NaCl, 10 mM $CaCl_2$, and 0.05% Brij (a nonionic detergent). All measurements were performed at 37.0°C.

Determination of kinetic parameters

The pre steady-state and steady-state parameters for the PSA-catalyzed hydrolysis of Mu-HSSKLQ-AMC were analyzed within the framework of the minimum three-step mechanism depicted by Figure 1: where E is the enzyme (*i.e.*, PSA), S is the fluorogenic peptide substrate (*i.e.*, Mu-HSSKLQ-AMC), ES is the enzyme-substrate complex, EP is the acyl intermediate, P_1 is AMC, P_2 is Mu-HSSKLQ, K_s is the fast pre-equilibrium constant (reflecting

$$E + S \underset{}{\overset{K_S}{\rightleftharpoons}} ES \xrightarrow{k_2} EP \xrightarrow{k_3} E + P_2 + P_1$$

Figure 2. Minimum three-step mechanism underlying the pre steady-state and steady-state parameters for the PSA-catalyzed hydrolysis of Mu-HSSKLQ-AMC.
doi:10.1371/journal.pone.0102470.g002

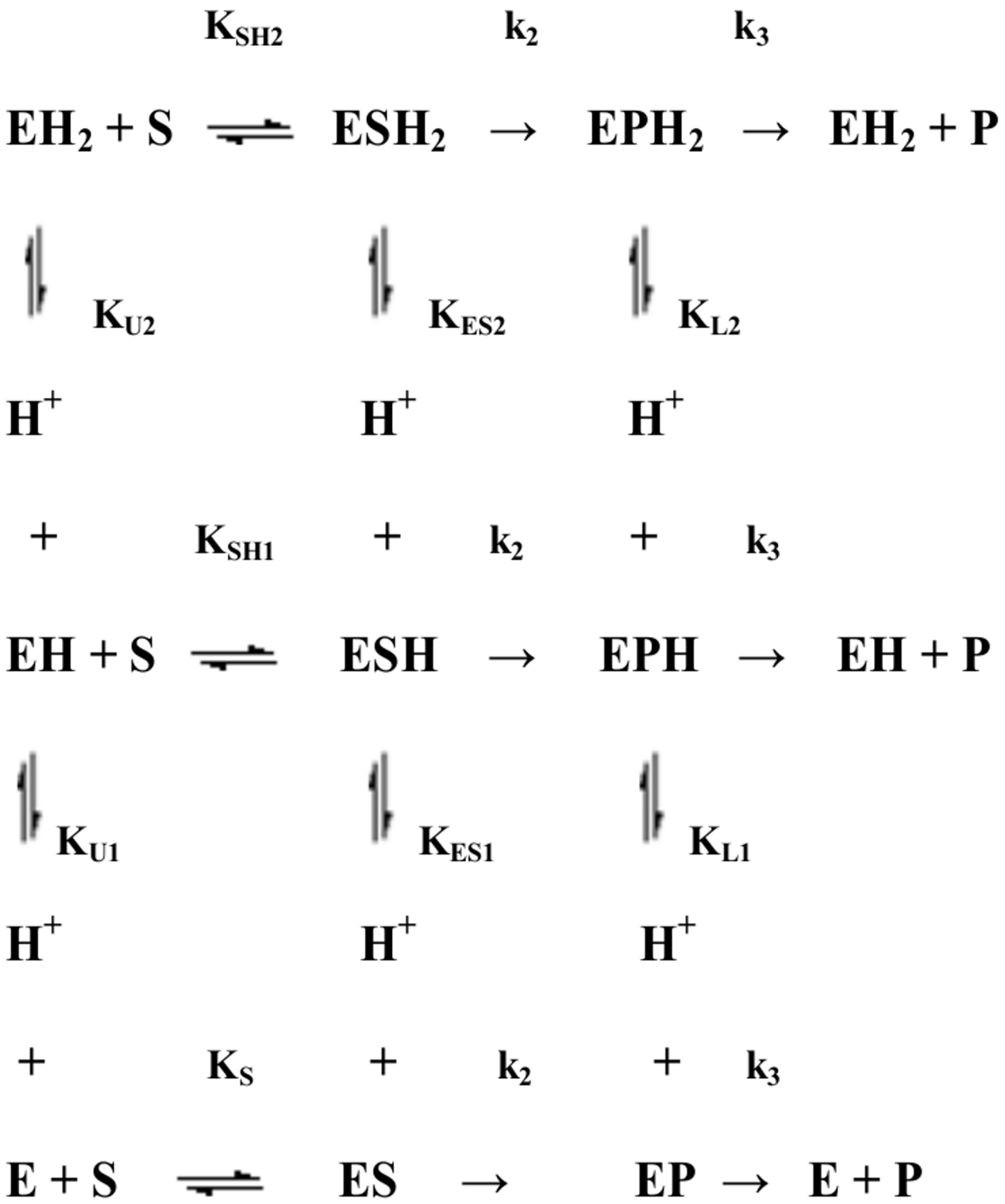

Figure 3. Minimum reaction mechanism for the pH dependence of pre-steady-state and steady-state parameters.
doi:10.1371/journal.pone.0102470.g003

the actual substrate affinity for the enzyme), k_2 is the acylation rate constant, and k_3 is the deacylation rate constant [19].

Since the fluorescence spectroscopic change is associated to the P_1 release, the enzymatic mechanism described in Figure 2 results in a biphasic kinetic pattern whenever $k_3 < k_2$ [19]. Therefore, P_1 release has been analyzed according to Eqn 1

$$[P_1] = \pi_0 \cdot \left(1 - e^{-k \cdot t}\right) + v \cdot t \quad (1)$$

where π_0 is the amplitude of the initial fast pre-steady-state phase

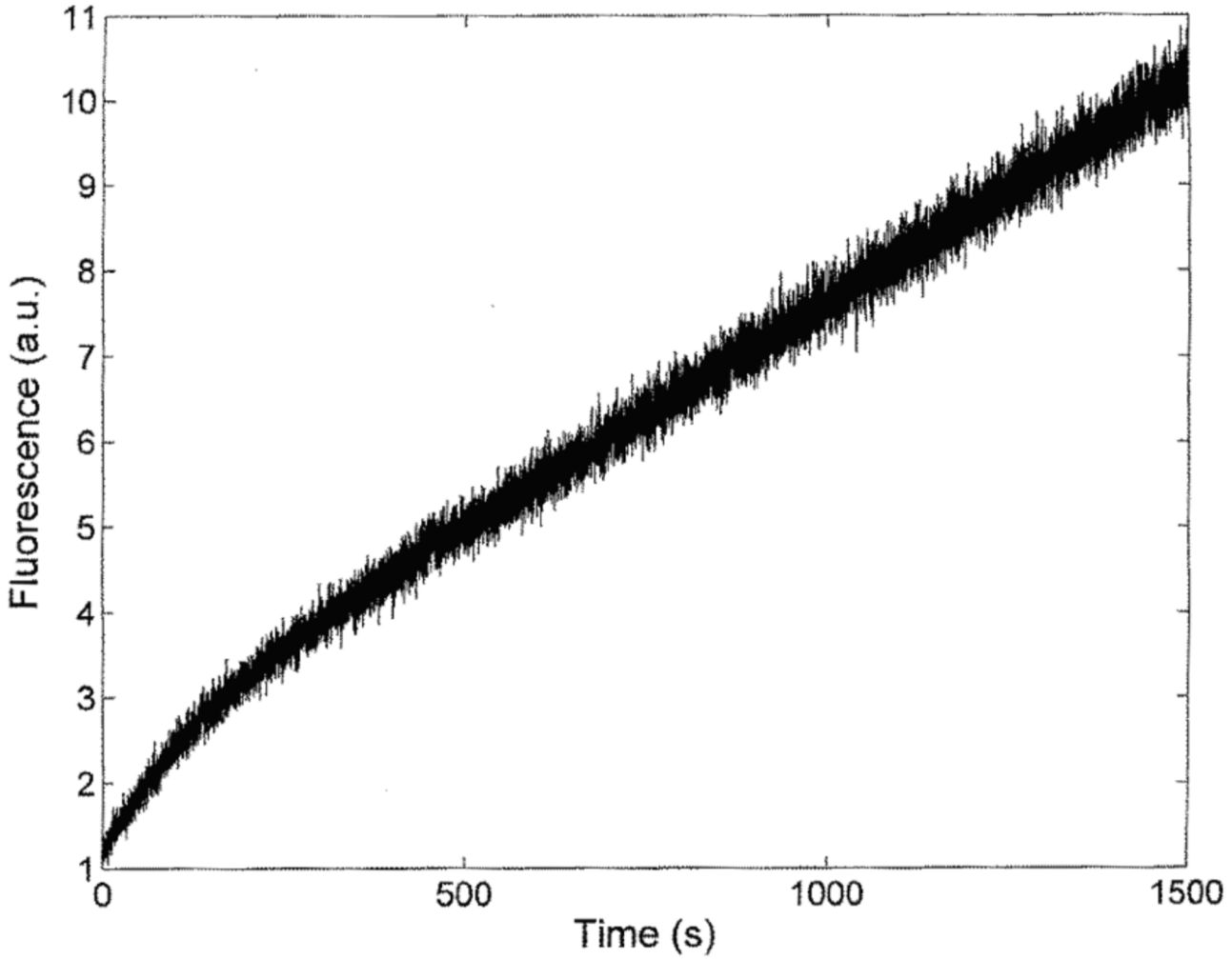

Figure 4. Time course of the PSA-catalyzed hydrolysis of Mu-HSSKLQ-AMC. Observation wavelength = 460 nm, pH = 7.5 and temperature = 37.0°C. The concentration of PSA was 50 nM. The concentration of Mu-HSSKLQ-AMC was 5 μM.
doi:10.1371/journal.pone.0102470.g004

(also known as the "burst"), k is the apparent rate constant of the initial fast pre-steady-state phase, ν indicates the subsequent slow steady-state process, and t is the time.

The initial fast pre-steady-state kinetics (see Eqn. 1) was analyzed according to Eqns 2 and 3 [20]:

$$\pi = [E]\cdot\left\{\frac{k_2\cdot[S]}{(k_2+k_3)\cdot(K_m+[S]}\right\}^2 \quad (2)$$

and

$$k = \frac{k_2\cdot[S]}{K_s+[S]} + k_3 \quad (3)$$

The analysis of kinetics according to Eqns. (2) and (3) allowed to determine the actual concentration of active PSA (*i.e.*, [E]) and values of K_s, k_2, and k_3.

The subsequent slow steady-state kinetics (see Eqn. 1) was analyzed according to Eqn. 4:

$$v = \frac{k_{cat}\cdot[E]\cdot[S]}{K_m+[S]} \quad (4)$$

where k_{cat} is the catalytic constant (corresponding to the rate-limiting step), K_m is the Michaelis constant, and [E] and [S] are the enzyme and substrate concentrations, respectively.

Of note, the steady-state parameters k_{cat} and K_m are related to the pre-steady-state parameters K_s, k_2, and k_3 according to Eqns 5 and 6:

$$k_{cat} = \frac{k_2\cdot k_3}{k_2+k_3} \quad (5)$$

and

$$K_m = \frac{K_s\cdot k_3}{k_2+k_3} \quad (6)$$

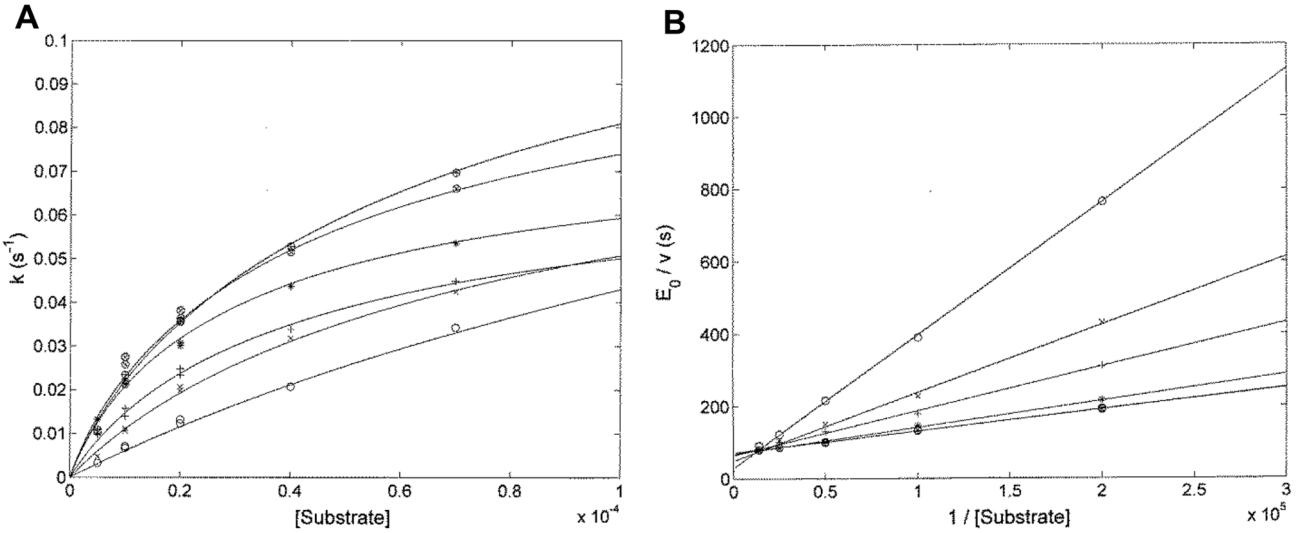

Figure 5. Dependence of *k* (panel A) and *v* (panel B) on the substrate concentration for the PSA-catalyzed hydrolysis of Mu-HSSKLQ-AMC. The continuous lines fitting the data reported in panels A and B were obtained according to Eqns. 3 and 4, respectively, with values of k_2, k_3, and K_s (panel A), and of k_{cat} and K_m (panel B) reported in Table 1. Values of pre-steady-state and steady-state parameters were obtained at pH 6.5 (o), pH 7.0 (x), pH 7.5 (+), pH 8.0 (*), pH 8.5 (:), and pH 9.0 (⊕) at a temperature of 37.0°C.
doi:10.1371/journal.pone.0102470.g005

The pH dependence of pre-steady-state and steady-state parameters was analyzed in the framework of the minimum reaction mechanism depicted in Figure 3 [21,22], where two protonating residues are involved, according to Eqns. 7-12:

$$^{obs}k_{cat} = {}^{0}k_{cat}\cdot\frac{1}{P_L} + {}^{1}k_{cat}\cdot\frac{K_{L1}\cdot[H^+]}{P_L} + {}^{2}k_{cat}\cdot\frac{K_{L1}\cdot K_{L2}\cdot[H^+]^2}{P_L} \quad (7)$$

$$^{obs}k_2 = {}^{0}k_2\cdot\frac{1}{P_{ES}} + {}^{1}k_2\cdot\frac{K_{ES1}\cdot[H^+]}{P_{ES}} + {}^{2}k_2\cdot\frac{K_{ES1}\cdot K_{ES2}\cdot[H^+]^2}{P_{ES}} \quad (8)$$

$$^{obs}k_3 = {}^{0}k_3\cdot\frac{1}{P_L} + {}^{1}k_3\cdot\frac{K_{L1}\cdot[H^+]}{P_L} + {}^{2}k_3\cdot\frac{K_{L1}\cdot K_{L2}\cdot[H^+]^2}{P_L} \quad (9)$$

$$^{obs}K_m = {}^{0}K_m\cdot\frac{1+K_{U1}\cdot[H^+]+K_{U1}\cdot K_{U2}\cdot[H^+]^2}{1+K_{L1}\cdot[H^+]+K_{L1}\cdot K_{L2}\cdot[H^+]^2} \quad (10)$$

$$^{obs}K_s = {}^{0}K_s\cdot\frac{1+K_{U1}\cdot[H^+]+K_{U1}\cdot K_{U2}\cdot[H^+]^2}{1+K_{ES1}\cdot[H^+]+K_{ES1}\cdot K_{ES2}\cdot[H^+]^2} \quad (11)$$

$$^{obs}(k_{cat}/K_m) = {}^{0}(k_{cat}/K_m)\cdot\frac{1}{P_U} + {}^{1}(k_{cat}/K_m)\cdot\frac{K_{U1}\cdot[H^+]}{P_U} + {}^{2}(k_{cat}/K_m)\cdot\frac{K_{U1}\cdot K_{U2}\cdot[H^+]^2}{P_U} \quad (12)$$

where

Table 1. Different parameters at various pH values, as obtained from the analysis of steady-state kinetics according to Eq. (1c) and of pre-steady-state kinetics according to Eq. (1d).

pH	k_{cat} (s^{-1})	K_m (M)	k_2 (s^{-1})	k_3 (s^{-1})	K_s (M)
6.5	$3.4(\pm0.5)\times10^{-2}$	$1.3(\pm0.3)\times10^{-4}$	$1.3(\pm0.3)\times10^{-1}$	$4.7(\pm0.6)\times10^{-2}$	$4.9(\pm0.6)\times10^{-4}$
7.0	$2.0(\pm0.3)\times10^{-2}$	$3.8(\pm0.5)\times10^{-5}$	$6.6(\pm0.9)\times10^{-2}$	$2.9(\pm0.5)\times10^{-2}$	$1.2(\pm0.3)\times10^{-4}$
7.5	$1.5(\pm0.3)\times10^{-2}$	$1.9(\pm0.3)\times10^{-5}$	$5.1(\pm0.7)\times10^{-2}$	$2.2(\pm0.4)\times10^{-2}$	$6.2(\pm0.8)\times10^{-5}$
8.0	$1.4(\pm0.3)\times10^{-2}$	$1.1(\pm0.2)\times10^{-5}$	$5.9(\pm0.9)\times10^{-2}$	$1.9(\pm0.3)\times10^{-2}$	$4.2(\pm0.7)\times10^{-5}$
8.5	$1.4(\pm0.3)\times10^{-2}$	$8.4(\pm1.1)\times10^{-6}$	$9.1(\pm1.7)\times10^{-2}$	$1.6(\pm0.3)\times10^{-2}$	$5.5(\pm0.9)\times10^{-5}$
9.0	$1.4(\pm0.2)\times10^{-2}$	$8.3(\pm1.0)\times10^{-6}$	$1.1(\pm0.2)\times10^{-1}$	$1.6(\pm0.3)\times10^{-2}$	$7.5(\pm1.0)\times10^{-5}$

doi:10.1371/journal.pone.0102470.t001

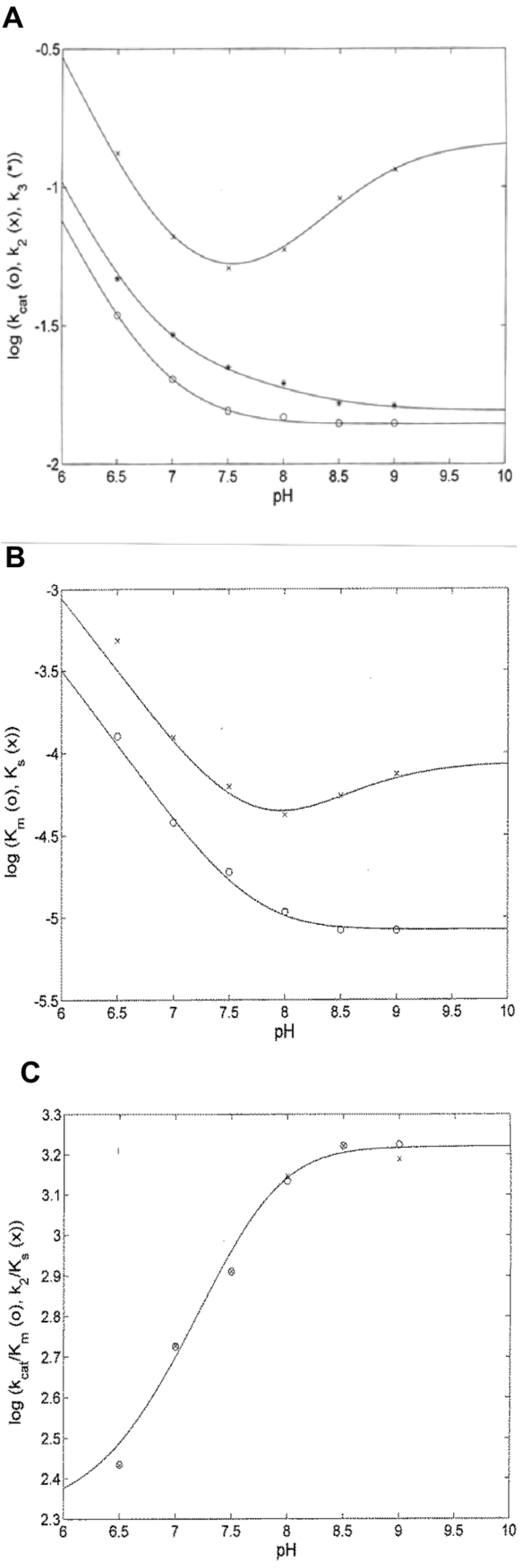

Figure 6. pH dependence of k_{cat} (o), k_2 (x), and k_3 (*) (panel A), of K_m (o) and K_s (x) (panel B), and of k_{cat}/K_m (o) and k_2/K_s (x) (panel C) for the PSA-catalyzed hydrolysis of Mu-HSSKLQ-AMC. The continuous lines have been obtained by non-linear least-squares fitting of data according to Eqs. 7–12 with parameters reported in Figure 6. The temperature was 37.0°C
doi:10.1371/journal.pone.0102470.g006

$$P_U = 1 + K_{U1}\cdot[H^+] + K_{U1}\cdot K_{U2}\cdot[H^+]^2 \quad (13)$$

$$P_{ES} = 1 + K_{ES1}\cdot[H^+] + K_{ES1}\cdot K_{ES2}\cdot[H^+]^2 \quad (14)$$

$$P_L = 1 + K_{L1}\cdot[H^+] + K_{L1}\cdot K_{L2}\cdot[H^+]^2 \quad (15)$$

${}^{obs}R$ refers to the observed parameter at a given pH value, ${}^{0}R$ refers to the parameter value of the unprotonated species, ${}^{1}R$ refers to the single-protonated species, and ${}^{2}R$ refers to the double-protonated species; K_{U1} and K_{U2} refer to the pK_a values (*i.e.*, $pK_{U1} = 10^{KU1}$ and $pK_{U2} = 10^{KU2}$) of protonating residues in the free enzyme, K_{ES1} and K_{ES2} refer to the pK_a values (*i.e.*, $pK_{ES1} = 10^{KES1}$ and $pK_{ES2} = 10^{KES2}$) of protonating residues in the ES complex and K_{L1} and K_{L2} refer to the pK_a values (*i.e.*, $pK_{L1} = 10^{KL1}$ and $pK_{L2} = 10^{KL2}$) of protonating residues in the EP form (see Figures 1 and 2).

Kinetics of the PSA-catalyzed hydrolysis of Mu-HSSKLQ-AMC were analyzed using the MatLab program (The Math Works Inc., Natick, MA, USA). The results are given as mean values of at least four experiments plus or minus the corresponding standard deviation.

Results and Discussion

Figure 4 shows a typical time course of the PSA-catalyzed hydrolysis of the fluorogenic substrate Mu-HSSKLQ-AMC (excitation wavelength = 380 nm; observation wavelength = 460 nm). This kinetic pattern, observed at all pH values, is characterized by the presence of the initial "burst" phase which precedes the insurgence of the steady-state phase. This feature, which can be described by Eqn 1, has been already observed for porcine pancreatic β-kallikrein [23] and it can be referred to a mechanism where the acylation and deacylation steps of the PSA-catalyzed hydrolysis of Mu-HSSKLQ-AMC (see Fig. 2) display different rate constants [19].

Figure 5 shows the substrate concentration dependence of k (according to Eqn, 3, see panel A) and v (according to Eqn. 4, see panel B), at different pH values. Of note, the two fitting procedures are interconnected and constrained according to the relationships depicted in Eqns. 3 and 4; therefore, they are mutually consistent, resulting in the parameters reported in Table 1.

The possibility of a quantitatively satisfactory description of the two processes by parameters which are mutually consistent indeed gives a great support to the fact that the mechanism described in Figure 2 is suitable to account for the observed behavior described in Figure 4. Furthermore, the difference between k_2 and k_3 at all investigated pH values (see Table 1) indicates that the rate-limiting step is not represented by the acylation reaction of the substrate (*i.e.*, the release of AMC, as observed in many proteolytic enzymes) [20], but it resides instead in the deacylation process (*i.e.*,

Table 2. pK$_a$ values from the pH-dependence of various kinetic parameters.

pK_{U1}	8.02±0.16
pK_{U2}	7.61±0.18
pK_{ES1}	8.59±0.17
pK_{ES2}	5.11±0.16
pK_{L1}	8.01±0.17
pK_{L2}	5.11±0.18

doi:10.1371/journal.pone.0102470.t002

the release of Mu-HSSKLQ) due to the low P_2 dissociation rate constant (*i.e.*, $k_2 \geq k_3 \approx k_{cat}$) (see Fig. 2).

Figure 6 shows the pH-dependence of the pre-steady-state and steady-state parameters for the PSA-catalyzed hydrolysis of Mu-HSSKLQ-AMC. The overall description of the proton linkage for the different parameters required the protonation/deprotonation of (at least) two groups with pK$_a$ values reported in Table 2. In particular, the different pK$_a$ values refer to either the protonation of the free enzyme (*i.e.*, E, characterized by pK_{U1} and pK_{U2}; see Fig. 3) or the protonation of the enzyme-substrate complex (*i.e.*, ES, characterized by pK_{ES1} and pK_{ES2}; see Fig. 3) or else the protonation of the acyl-enzyme intermediate (*i.e.*, EP, characterized by pK$_{L1}$ and pK$_{L2}$; see Fig. 3). The global fitting of the pH-dependence of all parameters according to Eqns. 7–12 allows to define a set of six pK_a values (*i.e.*, pK_{U1}, pK_{U2}, pK_{ES1}, pK_{ES2}, pK_{L1}, and pK_{L2}; see Table 2) which satisfactorily describe all proton linkages modulating the enzymatic activity of PSA and reported in Figure 3. Of note, all these parameters and the relative pK_a values are interconnected, since the protonating groups appear to modulate different parameters, which then have to display similar pK_a values, as indicated by Eqns. 7–12 (*e.g.*, pK_U's regulate K_m, K_s and k_{cat}/K_m, pK_{ES}'s regulate both K_s and k_2, and pK_L's regulate both K_m, k_3 and k_{cat}); therefore, pK$_a$ values reported in Table 2 reflect this global modulating role exerted by different protonating groups.

The inspection of parameters reported in Figure 7 envisages a complex network of interactions, such that protonation and/or deprotonation brings about modification of different catalytic parameters. In particular, the substrate affinity for the unprotonated enzyme (*i.e.*, E, expressed by $K_S = 8.8\times10^{-5}$ M; see Fig. 7) shows a four-fold increase upon protonation of a group (*i.e.*, EH, characterized by $K_{SH1} = 2.4\times10^{-5}$ M; see Fig. 7), displaying a p$K_a = 8.0$ in the free enzyme (*i.e.*, E, characterized by $K_{U1} = 1.1\times10^{8}$ M^{-1}; see Fig. 7), which shifts to p$K_a = 8.6$ after substrate binding (*i.e.*, ES, characterized by $K_{ES1} = 3.9\times10^{8}$ M^{-1}; see Fig. 7). On the other hand, this protonation process brings about a drastic five-fold reduction (from 0.15 s^{-1} to 0.036 s^{-1}; see Fig. 7) of the acylation rate constant k_2, which counterbalances the substrate affinity increase, ending up with a similar value of k_2/K_S (or k_{cat}/K_m) over the pH range between 8.0 and 9.0 (see Fig. 6, panel C). Because of this slowing down of the acylation rate constant (*i.e.*, k_2) in this single-protonated species, the difference with the deacylation rate is drastically reduced (thus $k_2 \approx k_3$; see Fig. 7). Further pH lowering brings about the protonation of a second functionally relevant residue, displaying a p$K_a = 7.6$ in the free enzyme (*i.e.*, E, characterized by $K_{U2} = 4.1\times10^{7}$ M^{-1}; see Fig. 7), which shifts to a p$K_a = 5.1$ upon substrate binding (*i.e.*,

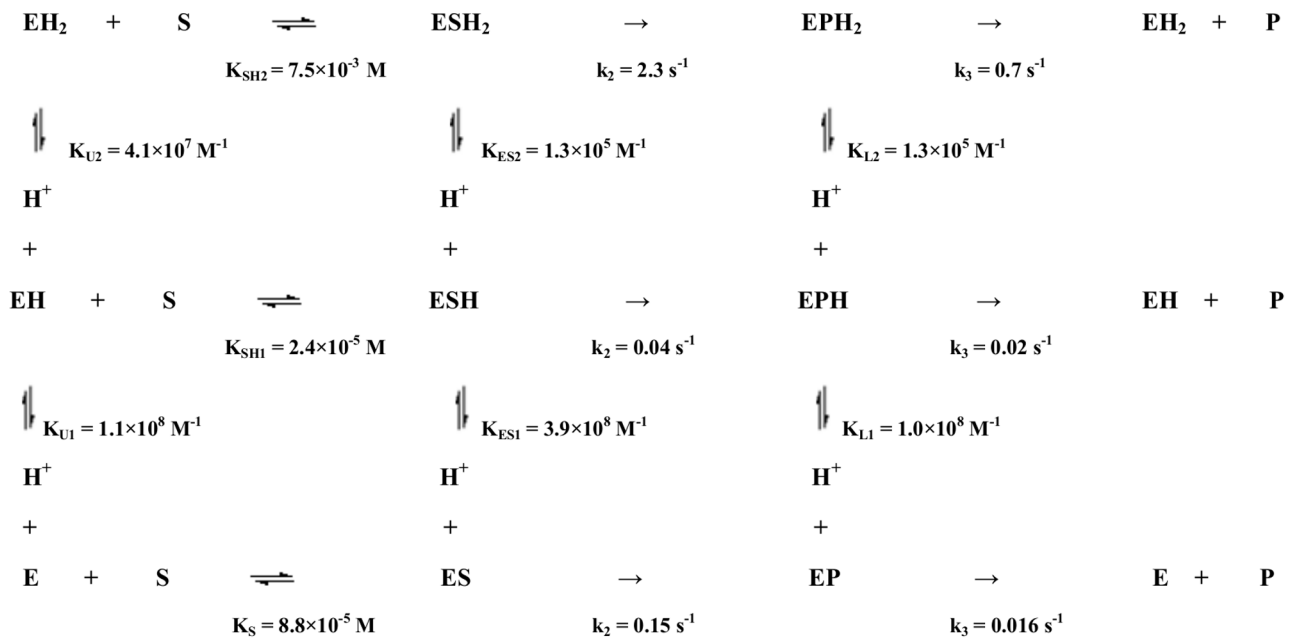

Figure 7. Proton-linked equilibria for the enzymatic activity of PSA at 37°C.
doi:10.1371/journal.pone.0102470.g007

$K_{ES2} = 1.3 \times 10^5$ M^{-1}; see Fig. 7). The protonation of this residue induces a drastic 250-fold decrease of the substrate affinity for the double-protonated enzyme (*i.e.*, EH_2, characterized by $K_{SH2} = 7.5 \times 10^{-3}$ M; see Fig. 7), even though it is accompanied by a 70-fold increase of the acylation rate constant k_2 ($= 2.3$ s^{-1}; see Fig. 7).

The identification of these two residues, characterized by substrate-linked $p\mathrm{K_a}$ shifts is not obvious, even though they are likely located in the kallikrein loop [24], which is known to restrict the access of the substrate to the active site and to undergo structural readjustment(s) upon substrate binding (see Fig. 1). In particular, a possible candidate for the first protonating residue ionizing at alkaline pH is the Lys95E of the kallikrein loop [24], which might be involved in the interaction with a carbonyl oxygen, orienting the substrate; this interaction could then distort the cleavage site, slowing down the acylation rate of the ESH (see Fig.7). On the other hand, the second protonating residue ionizing around neutrality may be a histidine (possibly even the catalytic His57), whose protonation dramatically lowers the substrate affinity, though facilitating the acylation step and the cleavage process. However, this identification cannot be considered unequivocal, since additional residues might be involved in the proton-linked modulation of substrate recognition and enzymatic catalysis, as envisaged in a structural modeling study [25], according to which, beside the His57 catalytic residue, a possible role might be played also by another histidyl group, possibly His172 (according to numbering in ref. [24]) (see Fig. 1).

Interestingly, after the acylation step and the cleavage of the substrate (with dissociation of the AMC substrate fragment), the $p\mathrm{K_a}$ value of the first protonating residue comes back to the value observed in the free enzyme, indeed suggesting that this ionizing group is interacting with the fluorogenic portion of the substrate which has dissociated after the acylation step (*i.e.*, P_1 in Figure 2), concomitantly to the formation of the EP complex; therefore this residue does not seem involved anymore in the interaction with the substrate, coming back to a situation similar to the free enzyme. On the other hand, the pK_a value of the second protonating residue ($= 5.1$) remains unchanged after the cleavage of the substrate observed in the EP complex, indicating that this group is instead involved in the interaction with the portion of the substrate which is transiently covalently-bound to the enzyme (possibly represented by the original *N*-terminus of the peptide), the dissociation (or deacylation) of the EP adduct representing the rate-limiting step in catalysis. Therefore, for this residue, ionizing around neutrality, the transformation of ES in EP does not bring about any modification of substrate interaction with the enzyme.

As a whole, from the mechanism depicted in Figure 7 it comes out that the enzymatic activity of PSA is mainly regulated by the proton-linked behavior of two residues, characterized in the free enzyme by $pK_{U1} = 8.0$ and $pK_{U2} = 7.6$, which change their protonation values upon interaction with the substrate. The evidence emerging is that these two residues interact with two different regions of the substrate, such that (*i*) the group characterized by pK_{U1}, which interacts with the portion released after the acylation process (probably corresponding to the original *C*-terminus of the substrate), displays a pK_a increase after substrate binding (likely reflecting the formation of an electrostatic favorable interaction in the ES complex), whereas (*ii*) the group characterized by pK_{U2}, which interacts with the portion released after the deacylation process, displays a $p\mathrm{K_a}$ decrease, clearly indicating that the corresponding residue tends to be deprotonated after substrate binding. The different modulatory role of the two residues, which sense in a distinct fashion the acylating and deacylating steps, is very interesting and may represent (i) an important mechanism to regulate in macromolecular substrates the release of different proteolytic products during the catalytic function of the enzyme and (ii) a relevant aspect to design enzyme inhibitors. In this respect, it is interesting to remark that the natural occurrence of a slow deacylating step in PSA might be exploited to design new potential inhibitors. Thus, appropriate modifications of the peptide sequence might be designed, so as to indefinitely slow down the deacylation step transforming he peptide in a "suicide" inhibitor, which completely abolishes the PSA activity.

Author Contributions

Conceived and designed the experiments: SM PA MC. Performed the experiments: LT DS MG ADM. Analyzed the data: LT DS MG ADM SM PA MC. Contributed reagents/materials/analysis tools: SM PA MC. Contributed to the writing of the manuscript: LT DS MG ADM SM PA MC.

References

1. Lilja H (1985) A kallikrein-like serine protease in prostatic fluid cleaves the predominant seminal vesicle protein. J Clin Invest 76: 1899–1903.
2. Ilic D, Neuberger MM, Djulbegovic M, Dahm P (2013) Screening for prostate cancer: an updated Cochrane systematic review. BJU International 107: 882–891.
3. Williams SA, Singh P, Isaacs JT, Denmeade SR (2007) Does PSA play a role as a promoting agent during the initiation and/or progression of prostate cancer? Prostate 67: 312–329.
4. Watt KW, Lee PJ, M'Timkulu T, Chan WP, Loor R (1986) Human prostate-specific antigen: structural and functional similarity with serine proteases. Proc Natl Acad Sci USA 83: 3166–3170.
5. LeBeau AM, Singh P, Isaacs JT, Denmeade SR (2009) Prostate-specific antigen is a "chymotrypsin-like" serine protease with unique P1 substrate specificity. Biochemistry 48: 3490–3496.
6. Denmeade SR, Sokoll LJ, Chan DW, Khan SR, Isaacs JT (2001) Concentration of enzymatically active prostate-specific antigen (PSA) in the extracellular fluid of primary human prostate cancers and human prostate cancer xenograft models. Prostate 48: 1–6.
7. Malm J, Hellman J, Hogg P, Lilja H (2000) Enzymatic action of prostate-specific antigen (PSA or hK3): substrate specificity and regulation by Zn(2+), a tight-binding inhibitor. Prostate 45: 132–139.
8. Suzuki K, Kise H, Nishioka J, Hayashi T (2007) The interaction among protein C inhibitor, prostate-specific antigen, and the semenogelin system. Semin Thromb Hemost. 33: 46–52.
9. Peter A, Lilja H, Lundwall A, Malm J (1998) Semenogelin I and semenogelin II, the major gel-forming proteins in human semen, are substrates for transglutaminase. Eur J Biochem 252: 216–221.
10. Edström AM, Malm J, Frohm B, Martellini JA, Giwercman A, et al. (2008) The major bactericidal activity of human seminal plasma is zinc-dependent and derived from fragmentation of the semenogelins. J Immunol 181: 3413–3421.
11. Cohen P, Graves HC, Peehl DM, Kamarei M, Giudice LC, et al. (1992) Prostate-specific antigen (PSA) is an insulin-like growth factor binding protein-3 protease found in seminal plasma. J Clin Endocrinol Metab 75: 1046–1053.
12. Iwamura M, Hellman J, Cockett AT, Lilja H, Gershagen S (1996) Alteration of the hormonal bioactivity of parathyroid hormone-related protein (PTHrP) as a result of limited proteolysis by prostate-specific antigen. Urology 48: 317–325.
13. Lilja H, Piironen TP, Rittenhouse HG, Mikolajczyk SD, Slawin KM (2000) Comprehensive Textbook of Genitourinary Oncology, Lippincott Williams and Wilkins, Philadelphia. pp 638–650.
14. Dallas SL, Zhao S, Cramer SD, Chen Z, Peehl DM, et al. (2005) Preferential production of latent transforming growth factor beta-2 by primary prostatic epithelial cells and its activation by prostate-specific antigen. J Cell Physiol 202: 361–370.
15. Webber MM, Waghray A, Bello D (1995) Prostate-specific antigen, a serine protease, facilitates human prostate cancer cell invasion. Clin Cancer Res 1: 1089–1094.
16. Ishii K, Otsuka T, Iguchi K, Usui S, Yamamoto H, et al. (2004) Evidence that the prostate-specific antigen (PSA)/Zn2+ axis may play a role in human prostate cancer cell invasion. Cancer Lett 207: 79–87.
17. Mattsson JM, Valmu L, Laakkonen P, Stenman UH, Koistinen H (2008) Structural characterization and anti-angiogenic properties of prostate-specific antigen isoforms in seminal fluid. Prostate 68: 945–954.

18. Denmeade SR, Lou W, Lovgren J, Malm J, Lilja H, et al. (1997) Specific and efficient peptide substrates for assaying the proteolytic activity of prostate-specific antigen. Cancer Res 57: 4924–4930.
19. Ascenzi P, Menegatti E, Guarneri M, Amiconi G (1989) Trypsin-like serine proteinase action: determination of the catalytic parameters K_S, k_{+2} and k_{+3} under conditions where the substrate exceeds the enzyme concentration. Biochim Biophys Acta 998: 210–214.
20. Antonini E, Ascenzi P (1981) The mechanism of trypsin catalysis at low pH. Proposal for a structural model. J Biol Chem 256: 12449–12455.
21. Gioia M, Fasciglione GF, Monaco S, Iundusi R, Sbardella D, et al. (2010) pH dependence of the enzymatic processing of collagen I by MMP-1 (fibroblast collagenase), MMP-2 (gelatinase A) and MMP-14 ectodomain. J Biol Inorg Chem 15: 1219–1232.
22. Petrera A, Amstutz B, Gioia M, Hähnlein J, Baici A, et al. (2012) Functional characterization of the *Mycobacterium tuberculosis* zinc metallopeptidase Zmp1 and identification of potential substrates. Biol Chem 393: 631–640.
23. Ascenzi P, Amiconi G, Bolognesi M, Guarneri M, Menegatti E, et al. (1984) The pH dependence of pre-steady-state and steady-state kinetics for the porcine pancreatic β-kallikrein-B-catalyzed hydrolysis of *N*-α-carbobenzoxy-L-arginine *p*-nitrophenyl ester. Biochim Biophys Acta 785: 75–80.
24. Menez R, Michel S, Muller BH, Bossus M, Ducancel F, et al. (2008) Crystal structure of a ternary complex between human prostate-specific antigen, its substrate acyl intermediate and an activating antibody. J Mol Biol 376: 1021–1033.
25. Singh P, LeBeau AM, Lilja H, Denmeade SR, Isaacs JT (2009) Molecular insights into substrate specificity of prostate specific antigen through structural modeling. Proteins 77: 984–993.
26. Pettersen EF, Goddard TD, Huang CC, Couch GS, Greenblatt DM, et al. (2004) UCSF Chimera - a visualization system for exploratory research and analysis. J Comput Chem 25: 1605–1612.
27. Tang J, Yu CL, Williams SR, Springman E, Jeffery D, et al. (2005) Expression, crystallization, and three-dimensional structure of the catalytic domain of human plasma kallikrein. J Biol Chem 280: 41077–41089.
28. Fernández IS, Ständker L, Mägert HJ, Forssmann WG, Giménez-Gallego G, et al. (2008) Crystal structure of human epidermal kallikrein 7 (hK7) synthesized directly in its native state in E. coli: insights into the atomic basis of its inhibition by LEKTI domain 6 (LD6). J Mol Biol 377: 1488–1497.